Available online at www.jobpcr.com

ISSN-2394:3076
CODEN(USA) : JBPCBK
Journal of Biological Pharmaceutical And Chemical Research, 2014,1(1): 192-204

(http://www.jobpcr.com/arhcive.php)

Assessing the Effect of Matrix Metalloproteinase-9 on the Growth of Mice Teeth by NMR

Qingwen Ni[1,2*] , Shuo Chen[3]
[1]*Texas A&M International University, TX, USA*
[2]*Southwest Research Institute, TX, USA*
[3]*The University of Texas Health Science Center, TX, USA*

ABSTRACT

A wide spectrum of mouse and human disorders affecting tooth and bone biomineralization shows that dentin and bone formation are under strict genetic control. Although the controlling mechanisms of dentinogenesis and osteogenesis require further study, a large body of evidence points to the importance of the matrix metalloproteinases (MMPs) participate in a wide variety of extracellular matrix degradation. Currently, we attempt to find that in MMP-9 knock out (KO) mice displayed severe attrition on teeth development. In this study a technique of low-field nuclear magnetic resonance (NMR) spin relaxation (T_2) is applied for assessment of MMP-9 KO mice and wild-type (normal). Then, the spin relaxation decay curve is converted into T_2 distribution spectrum. Here, we propose an NMR "calibration method" – the ratio of the amount of fluid in pulp component to the amount of fluid in dentin component obtained from NMR T_2 distribution spectra. This ratio method can be used to calibrate the age-growth MMP-9 KO structural changes in teeth while eliminating any variations in size of teeth. Five MMP-9 KO groups from 10 days to 147 days were tested in this study. It is found that the ratio of dental pulp chamber to dentin greatly varies on the early age periods (1 month) than on the elder ages suggesting that MMP-9 is more involved in early stages of tooth development and formation.

Keywords : MMP-9, teeth, NMR, x-ray.

INTRODUCTION

Matrix metalloproteinases (MMPs), a family of zinc-dependent endopeptidases, are able to degrade all extracellular matrix proteins [1]. The MMPs can be classified into collagenases, gelatinases, stremelysins, membrane-type MMP, minimal-domain MMPs, and others. Two gelatinases (MMP-2 and MMP-9) are capable of degrading gelatins, lamin, elastin, fibronectin, and basement membrane zone-associated collagen [2]. They are involved in the normal turnover of extracellular matrix (ECM). The proteolysis of ECM seems to be a key initiating event for progression of the inflammatory process, such as rheumatoid arthritis and periodontitis [3].

Recently, studies have been shown that MMPs play an important role in tissue degradation in inflammatorydental pulp [4-9]. In addition, MMP-9 was found to be upregulated in inflammatory pulp tissues by gelatin zymography [10]. The data obtained suggest a key role of MMP-9 in the

breakdown of human dental pulp tissue. However, these studies do not reveal the cellular sources of MMP-9 in clinically healthy pulps as well as inflammatory dental pulps. The physical and chemical properties of dentin closely resemble those of bone. On the other hand, bone and dentin have obvious morphological differences. Thus, it is unclear whether the process of osteoclastic bone resorption is similar to or different from the removal of dental hard tissue by odontoclasts.

Bone remodeling is a dynamic process that involves bone resorption and formation. Unlike bone remodeling, physiological root resorption occurs only during the shedding of deciduous teeth. However, bone resorption and root resorption are similar in that both involve decalcification of mineral crystals in an acidic microenvironment and degradation of the organic matrix by proteinases. Both in vitro and in vivo studies have suggested that the degradation of bone collagen by osteoclasts mainly involves two types of proteinases, the MMPs and lysosomal cysteine proteinases [11-19]. Among the MMPs, MMP-9 (gelatinase B, a 92 kDa type IV collagenase) has been shown to be abundantly expressed by osteoclasts in mouse, rabbit, and human bone tissues [18, 21-23] and in multinucleated giant cells of human osteoclastomas. Previous reports have noted that MMP-9 may be expected to play a role in the removal of denatured collagen fragments following the action of other MMPs and cysteine proteinases during osteoclastic bone resorption. Furthermore, MMPs are indispensable for the recruitment of osteoclasts [24] and this role is distinct from synergy with cysteine proteinases in solubilizing calcified matrix in the resorption zone [12, 25]. It was recently shown that MMP-9 is a major MMP for this recruitment process [26]. This role of MMP-9 is supported by the observation that mice deficient in MMP-9 exhibit a delay in osteoclast recruitment [26].

Detailed knowledge of MMPs may be important for understanding the pathogenesis of tooth development. Some researchers have pointed MMP-9 is an extracelluar proteinase that is highly expressed in osteoclasts and has been postulated to play an important role in their resorptive activity. Although MMP-9 has been reported to play a role in bone resorption, the association of this enzyme during deciduous tooth resorption has not yet been clarified. Based on accumulating evidence, we hypothesized that MMP-9 should play a role in teeth formation and development. However, there is no information available regarding the presence and function of MMP-9 in teeth formation.

In this study, we applied NMR relaxation technique to assess age-related MMP-9 knock out (KO) tooth quality *in vitro* by quantifying changes in dentin and pulp simultaneously. The major hypothesis in this paper was that whether noninvasive NMR relaxation time measurements could be used to characterize MMP-9 KO changes in dentin and pulp, and to predict tooth quality. Specifically, we tested that age-related MMP-9 KO tooth changes result in an alteration of the NMR spin-spin (T_2) relaxation time signal due to the structural changes in the tooth matrix. This signal can be further processed to produce a T_2 relaxation distribution spectrum related to dentin and pulp, and their derived parameters can be used as descriptors of age-related MMP-9 KO tooth changes. In this study, the proton liquid-like NMR spin-spin (T_2) relaxation decay signal was obtained from the Carr-Purcell-Meiboom-Gill (CPMG) NMR spin echo train method [32,33], then the relaxation decay signal was converted to T_2 relaxation distribution spectra describing the size domain of dentin and pulp. Therefore, we can calibrate the intensities in NMR inversion T_2 relaxation distribution spectra corresponding to the amount of dentin and pulp related to the structural changes.

Here, we propose an NMR calibration method “NMR standard estimation” – the ratio of the amount of fluid in pulp component to the amount of fluid in dentin component obtained from NMR T_2 distribution spectra that can be used to measure the age-related MMP-9 KO structural changes in

teeth. We are cognizant of the biological and physiological variability manifest in teeth size variations, but demonstrated that this kind of NMR standard estimation – the ratio of amount of dentin to amount of pulp from the NMR T_2 inversion spectrum can be used to determine age-related MMP-9 KO structural changes in teeth and eliminate any variations in size of teeth.

MATERIALS AND METHOD

Sample Population and Preparation

All experimental procedures involving the use of animals were reviewed and approved by the Institutional Animal Care at the University of Texas Health Science Center at San Antonio, TX (UTHSCSA). The MMP-9 knockout mice were generated as described previously [35]. In brief, the mouse MMP-9 gene was cloned from a 129/Sv genomic library in a bacteriophage P1 vector. A targeting construct was generated in pBluescript SK that included 5.3 kb of 5' homology and 3.1 kb of promoter sequence, exon 1, intron 1, and 28 bp of exon 2. A cassette containing the neomycin phosphotransferease cDNA driven by the phosphoglycerate kinase promoter (PGK-Neo was used to replace most of exon 2 and all of intron2. Targeting construct was lineralized with NotI prior to electroporation into embryonic stem cells. The targeted embryonic stem cell clones were injected into blastocysts of C56BL/6J mice and transferred into uteri of pseudopregnant females, and offspring were screened by PCR of tail genomic DNA and gelatin SDS-substrate gel zymorgraphy. The PCR primers used for genotyping of MMP-9 gene were as follows: wild type; forward, 5'-GCA TAC TTG TAC CGC TAT GG-3'; reverse, 5'-TAA CCG GAG GTG CAA ACT GG-3'; mutant; 5'-CTC AGA AGA ACT CGT CAA GA-3' reverse, GGA TTG CAC GCA GGT TCT CC-3'. The cycle paprameters were: 94^{o}C for 15 min, followed by 32 cycles of 94^{o}C for 1 min, 58^{o}C for 1 min, and 72^{o}C for 1 min, final on cycle of 72^{o}C for 5 min. The PCR products were run on 1% agarose gels and stained with Ethidium bromide. Once MMP-9 deletion was confirmed, mice were examined to identify signs of defective craniofacial and tooth functions.

Approximately 30 mice with MMP-9 KO and 5 wild-type mandibles (30-day-old) were collected and used from UTHSCSA. The MMP-9 KO species are divided into 5 groups: 10 days, 15 days, 30 days, 45 days and 147 days. Any soft tissue attachment was carefully cleaned up from the surface of the mandibular tooth samples. All the specimens were stored in phosphate-buffered-saline solution at -5 C^o.

Experimental Studies

A Bruker Minispec NMR system was set up at a proton frequency of 20 MHz for these measurements. ^{1}H spin-spin (T_2) relaxation profiles were obtained by using NMR CPMG[32, 33] $\{90^0 [- \tau - 180^0 - \tau (\text{echo})]_n - T_R\}$ spin echo method with a 6.9 μs wide RF-90^o pulse, τ of 250 μs, and T_R (sequences repetition rate) of 15 s. After NMR measurements the samples were done by X-ray measurements.

Also, the experimental studies were used for assignments of two peaks in NMR inversion T_2 spectra (Figure 2). In our previous NMR on tooth study, it was provedthat there were two peaks in NMR inversion T_2 spectra [34]. Therefore, it can be assumed that the first peak (from left to right) is due to fluid within the pores in dentin like component, and the second peak is due to the fluid within pulp like cavity in the mandibular samples. This is proved by NMR measurements on using dentin component only, or pulp cavity only samples, respectively [34].

Relationship between NMR Data and Pore Size

The essential feature for an NMR experiment is that the transient NMR signal from solids decay

very fast (decay time constant T_2 is normally less than 100 μs), while it takes much longer to decay in liquids. In porous media, using NMR CPMG sequence measurement, the total amplitude of the transient hydrogen NMR signal is representative of the liquid phase inside the pores [32, 33]. In low-field NMR, at the fast diffusion limit (diffusion effect is negligible), the relaxation rate $1/T_2$ is proportional to the surface-to-volume (S/V) ratio of the pore [29]:

$$1/T_2 = \rho\,(S/V)_{pore} \qquad (1)$$

where ρ is the surface relaxivity– a measure of the pore surface's ability to enhance the relaxation rate – which falls within a reasonably narrow band. For compact bone material, it ranges roughly from micron to tens of microns per second [18, 29].

In the NMR CPMG [32,33] sequence (90^0 - t - 180^0 - echo - delay) for spin-spin relaxation measurement, for a fluid contained in a single pore size, the echo following the 180^0 rotation of the magnetization vector is given by

$$M(t) = M_o\exp(-t/T_2) \qquad (2)$$

where M_o is the magnetization of the nuclei at equilibrium and M(t) is the observed magnetization at a variable delay time t, between the 90^o and 180^o measurement pulses. For porous teeth, the observed nuclear magnetization (NMR signal) depends on the T_2 (i.e., pore size) of all pores. As shown in Equation (1), the NMR relaxation time is proportional to pore size, and it is known that teeth and bones have distributions of pore sizes. This implies that NMR transverse relaxation (T_2) data can be expressed as a sum of exponential functions:

$$M(t) = \sum_I M_i\exp(-t/T_{2i}) \qquad (3)$$

where M_i is proportional to the number of spins that relax with a time constant T_{2i}. M(t) is the NMR magnetization decay from fluid saturated teeth and compact bone. Equation (3) can be inverted into a T_2 relaxation time distribution. Thus, instead of estimating a single relaxation time from a magnetization decay, it is necessary to estimate a spectrum or distribution of relaxation times $M(T_{2i})$. Since T_2 depends linearly on pore size, the T_2 distribution corresponds to pore-size distribution, with the longer relaxation times being from larger pores [28,30].

Ratio of NMR T_2 Inversion Spectral Peak Intensity

Here, we propose an NMR "calibration method"– the ratio of the amount of fluid in pulp like component (second peak) to the amount of fluid in dentin like component (first peak) obtained from NMR T_2 distribution spectra that can be used to measure the structural changes due to MMP-9 knock off in teeth. We are cognizant of the biological and physiological variability manifest in teeth size variations, but feel that this kind of NMR standard estimation – the ratio of amount of pulp to amount of dentin from the NMR T_2 inversion spectrum can be used to determine MMP-9 knock-off structural changes in teeth and eliminate any variations in size of teeth.

RESULT AND DISCUSSION

Figure 1 shows an example of NMR CPMG relaxation decay data for normalized signals (assuming from the same volume) for the 45-day-old first mandibular molars of the wide-type and MMP-null mice plotted in a linear scale, respectively indicating multiexponential relaxation behavior. The intensity differences between them are proportional to the total liquid-like (mobile water) proton magnetization differences.

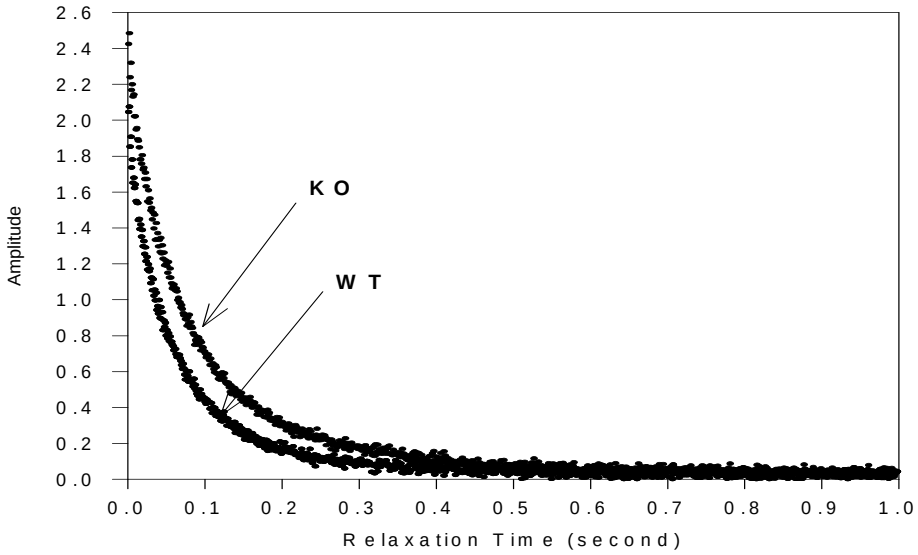

Figure 1. NMR CPMG spin relaxation decay data from 45-day-old first mandibular molars of the wide-type (low amplitude) and MMP-9 null mice (higher amplitude) plotted in a linear scale, respectively. Both signals show multiexponential relaxation behavior.

Using the T_2 relaxation decay data shown in Figure 1 the inversion T_2 relaxation distribution patterns for these two specimens are shown in Figure 2. The longer relaxation time (T_2) is corresponding to larger pores, and the larger areas (under the curve) is corresponding to larger porosity (larger amount of holes).

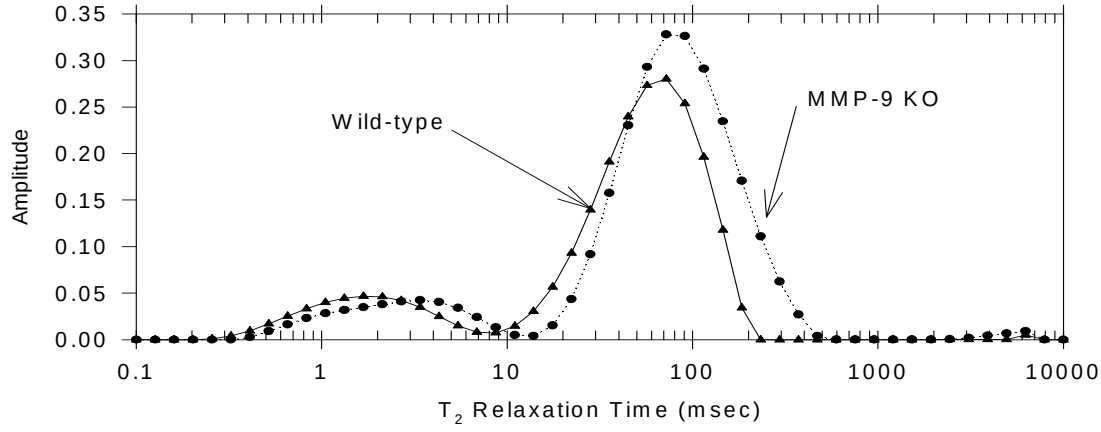

Figure 2. Comparison of inversion of T_2 relaxation time spectra for the 45-day-old first mandibular molars of the wide-type and MMP-null mice.

Figures 3 to 5 show the examples of NMR CPMG relaxation decay data and its T_2 inversion

relaxation spectra from wide type (30 days), MMP-9 knock out (30 days), and MMP-9 knock out (147 days), respectively.

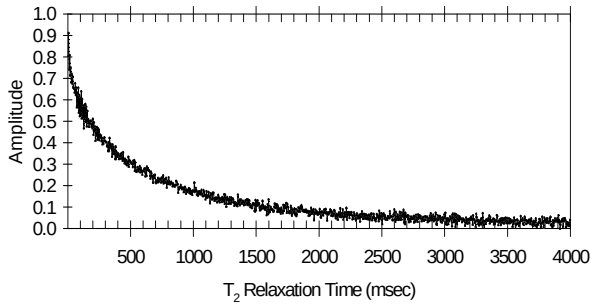

Figure 3a. NMR CPMG spin relaxation (T2) data from first mandibular molars of wide type mice (30-day-old).

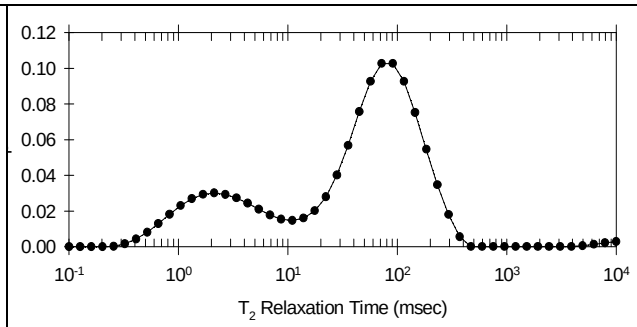

Figure 3b. NMR inversion T2 spin relaxation data from first mandibular molars of wide type mice(30-day-old).

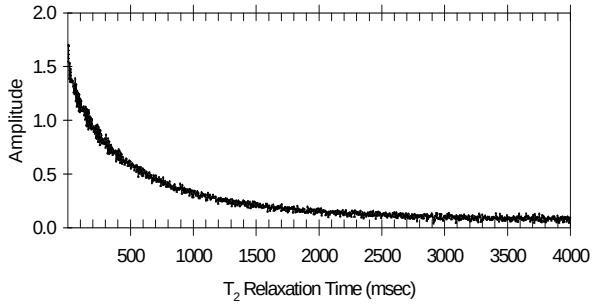

Figure 4a. NMR CPMG spin relaxation (T2) data from first mandibular molars of mice after 30 days MMP-9 KO.

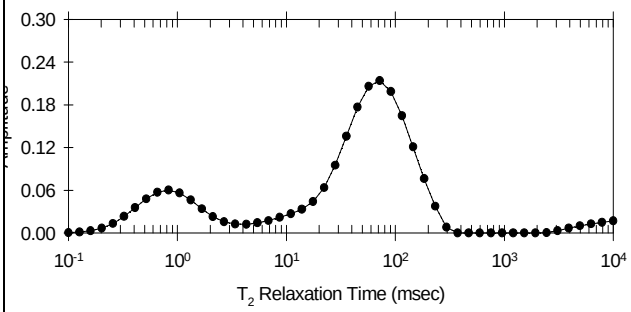

Figure 4b. NMR inversion T2 spin relaxation data from first mandibular molars of mice after 30 days MMP-9 KO.

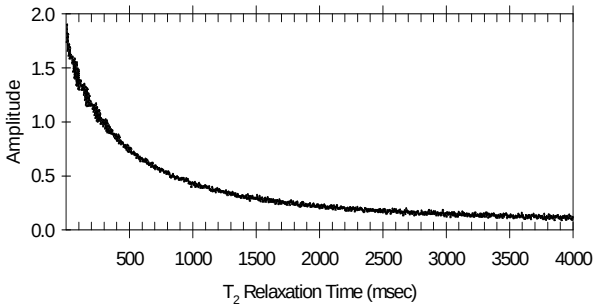

Figure 5a. NMR CPMG spin relaxation (T2) data from first mandibular molars of mice after 147 days MMP-9 KO.

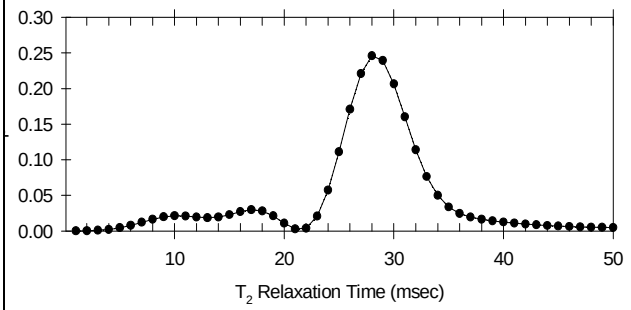

Figure 5b. NMR inversion T2 spin relaxation data from first mandibular molars of mice after 147 days MMP-9 KO.

Figures 6-8 show the X-ray images for the 15-, 45- , and 147-day-old first mandibular molars of the wide-type and MMP-null mice. The morphology difference between them is observed. And Figure 9 shows the changes of dentin thickness and dental pulp cavities for a 45-day-oldfirst mandibular molar with and without MMP-9 null mouse.

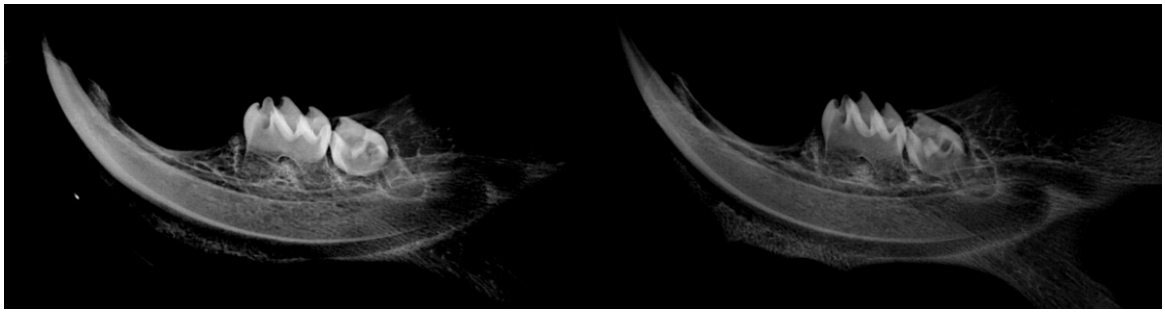

Figure 6. Comparison of the X-ray images for the 15-day-old first mandibular molars of the wide-type and MMP-null mice; left: wild-type; right: MMP-9 null.

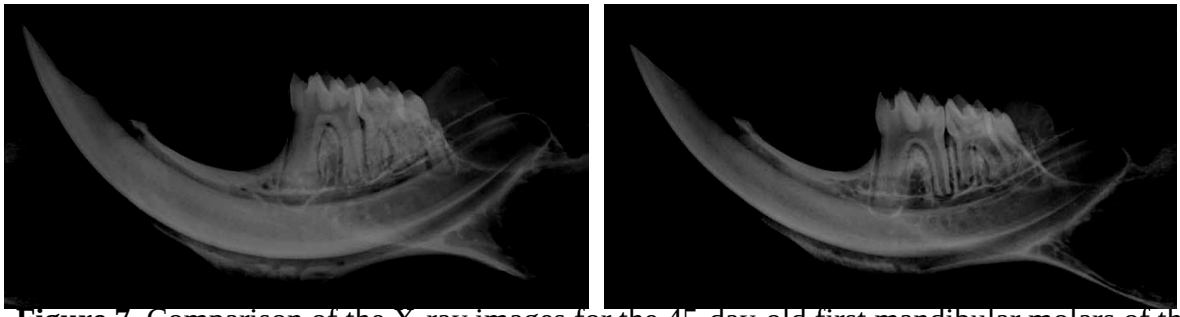

Figure 7. Comparison of the X-ray images for the 45-day-old first mandibular molars of the wide-type and MMP-null mice; left: wild-type; right: MMP-9 null.

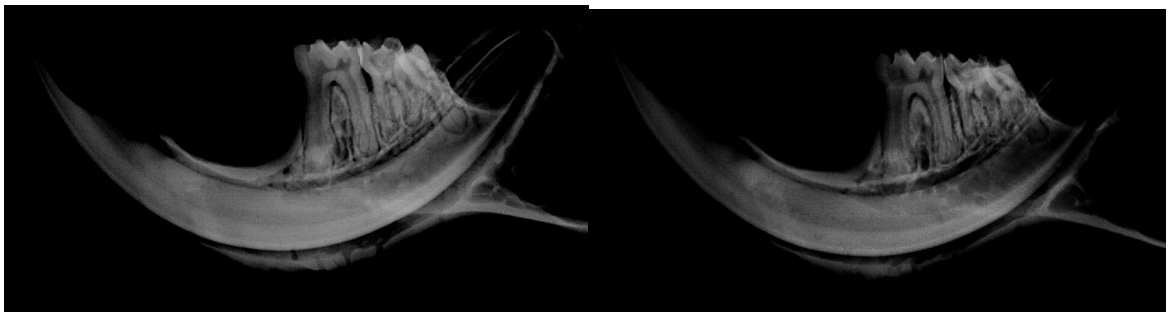

Figure 8. Comparison of the X-ray images for the 147-day-old first mandibular molars of the wide-type and MMP-null mice; left: wild-type; right: MMP-9 null.

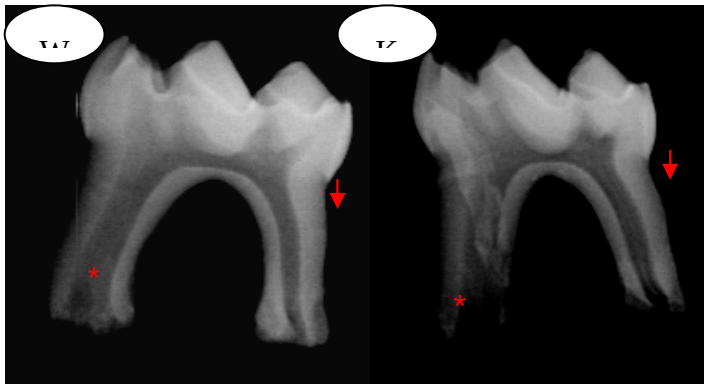

Figure 9. Decreased dentin thickness and increased dental pulp cavities on a 45-day-old first mandibular molar of MMP-9 null mouse compared to the wild-type.

In addition, the representative radiograph of mandibles in Figure 9 shows a lower mineralization with enlarged dental pulp cavity in MMP-9 KO mice (arrows). These are consistent with NMR spectra.

Figure 10 and 11 show the absolute unit for the areas under the curve from Figure 3b and 5b, respectively by using SigmaPlot Peak Fit Program. The estimated average intensity ratios of the second peak (pulp like component) to the first peak (dentin like component) from 10-, 15-, 30-, 45-, and 147-day-old MMP-9 KO, and comparison with wide-type teeth (30 days) are shown in Table 1.

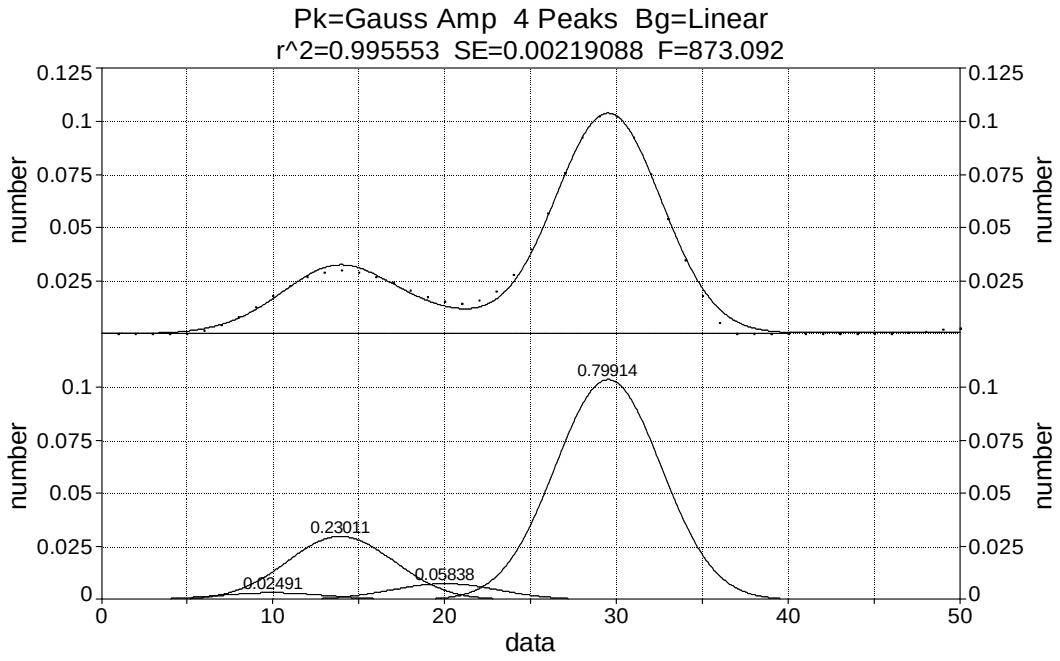

Figure 10. The estimated absolute unit under the curve from Figure 3b (wide-type).

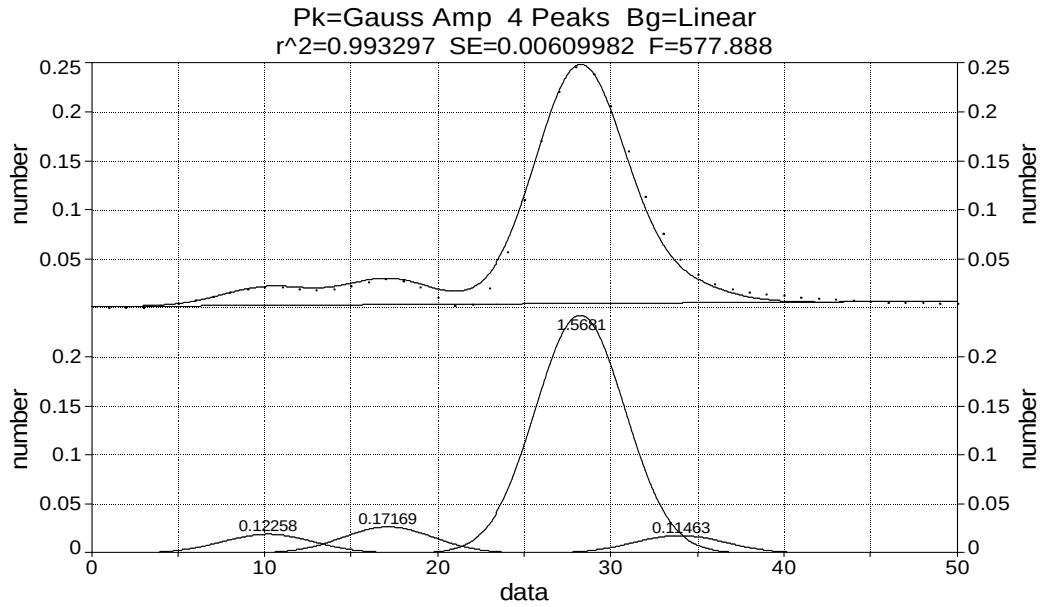

Figure 11. The estimated absolute unit under the curve from Figure 8b (MMP-9 null).

Table 1. The estimated average intensity ratios of the second peak (pulp) to the first peak (dentin) from MMP-9 KO and wide-type teeth.

Sample	Area Peak 1	Area Peak 2	Ratio 2:1
WT1 (D30)	0.29575	0.76506	2.5868
WT2 (D30)	0.29394	0.81855	2.7849
WT3 (D30)	0.21403	0.72640	3.3940
WT4 (D30)	0.31063	0.92348	2.9729
WT5 (D30)	0.26053	0.63052	2.4201
Average			**2.8317±0.4053**
D10_1	0.32810	0.89077	2.7149
D10_2	0.28719	0.86237	3.0028
D10_3	0.30574	1.03615	3.3890
D10_4	0.25731	0.81784	3.1784
D10_5	0.31527	0.85181	2.7018
Average			**2.9974±0.2972**
D15_1	0.41226	1.94383	4.7151
D15_2	0.36110	1.29400	3.5835
D15_3	0.32308	0.83072	2.5713
D15_4	0.29922	0.94502	3.1583
D15_5	0.20019	0.64155	3.2047
Average			**3.4466±0.7962**
D30_1	0.46408	2.16104	4.6566
D30_2	0.56797	1.56520	2.7558
D30_3	0.30705	0.94264	3.0700
D30_4	0.29086	0.81350	2.7969
D30_5	0.18367	0.78807	4.2907
Average			**3.5140±0.8937**
D45_1	0.31083	1.33421	4.2924
D45_2	0.24990	0.98051	3.9237
D45_3	0.26432	0.77089	2.9165
D45_4	0.32956	1.04522	3.1715
Average			**3.5760±0.6410**
D147_1	0.29427	1.2014	4.1079
D147_2	0.19981	0.81782	4.0930
D147_3	0.21415	0.7310	3.4139
D147_4	0.20920	0.6994	3.3430
Average			**3.7395±0.4179**

Therefore, the X-ray image can provide the quality information related to the morphology changes from the wide-type and the MMP-null mice. NMR inversion spectra can provide the quantitative difference between these types of teeth. The changes between the average intensity ratios of pulp peak to dentin peak vs. the days are plotted in Figure 12.

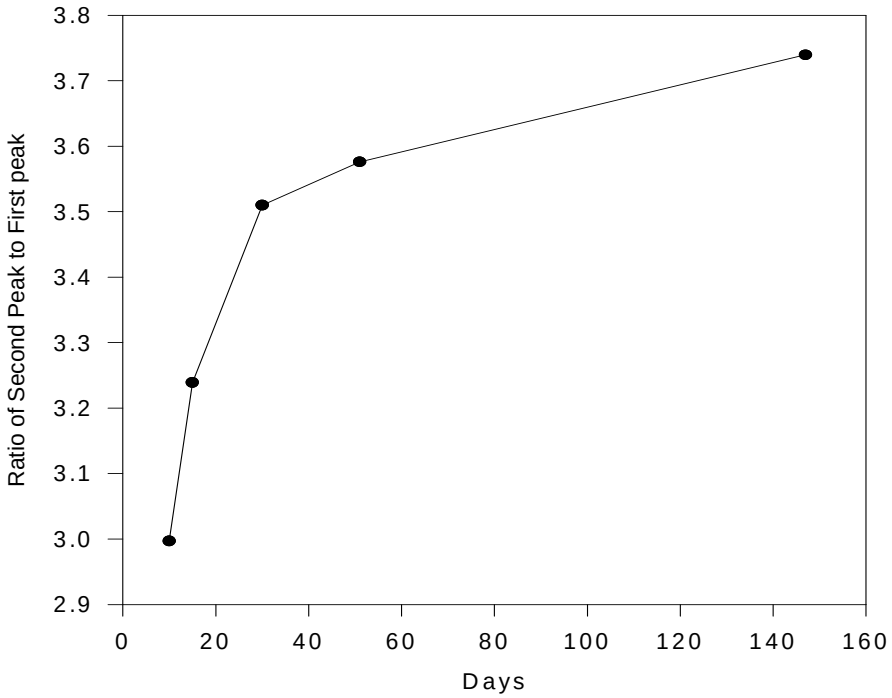

Figure 12. The intensity ratio of pulp peak to dentin peak vs. the days of MMP-9 KO.

The plot evidently shows that ratio of dental pulp chamber to dentin greatly varies on the early age periods (1 month) between the wild-type and MMP-9 groups, while there are less variations of the ratio of the dental pulp chamber to dentin of the two groups, suggesting that MMP-9 is involved in early stages of tooth development and formation.

CONCLUSION

Using a technique of low-field pulsed proton nuclear magnetic resonance (NMR) spin relaxation, we observed different ratio of dentin and dental pulp chamber between the wild-type and MMP-9 KO mice. The NMR result is similar to that of X-ray image. X-ray image can provide the quality information related to the morphology changes from the wide-type and the MMP-null mice. However, NMR inversion spectra can provide the quantitative difference between these types of teeth. The NMR is a rapid, non-destructive and non-invasive technique, so that this technique can be used to analyze micro-structural changes in teeth and other tissues in physiological and pathological activity.

ACKNOWLEDGEMENTS

This work was support by internal research project of SwRI, TAMIU and UTHSCSA.

REFERENCES

[1] WD Sternlicht and Z Werb, How matrix metalloproteinases regulate cell behavior, *Annu Rev Cell Dev Biol* 17 , **2001;** pp. 463–516.b

[2] Z Werb, Proteinases and matrix degradation. In: WN Kelly, FD Harris Jr, S Ruddy and CB Sledge, Editors, *Textbook of rheumatology* (3rd ed.), Saunders, Philadelphia, **1989**; pp. 300–321.

[3] JF Woessner Jr, Matrix metalloproteinases and their inhibitors in connective tissue remodeling, *FASEB*5, **1991**; pp. 2145–2154

[4] FS Panagakos, JF O'Boskey Jr and E Rodriguez, Regulation of pulp cell matrix metalloproteinases production by cytokines and lipopolysaccharides, *J Endod* 22, **1996**;pp. 358–361.

[5] JF O'Boskey Jr and FS Panagakos, Cytokines stimulate matrix metalloproteinases production by human pulp cells during long-term culture, *J Endod* 24, **1998**; pp. 7–10.

[6] YC Chang, SF Yang and YS Hsieh, Regulation of matrix metalloproteinases-2 production by cytokines and pharmacological agents in human pulp cell cultures, *J Endod* 27, **2001**; pp. 679–682.

[7] YC Chang, CC Lai, SF Yang, Y Chan and YS Hsieh, Stimulation of matrix metalloproteinases by black-pigmented *Bacteroides* in human pulp and periodontal ligament cell cultures, *J Endod* 28 , **2002**; pp. 90–93.

[8] FM Huang, SF Yang, YS Hsieh, CM Liu, LC Yang and YC Chang, Examination of the signal transduction pathways involved in matrix metalloproteinases-2 in human pulp cells, *Oral Surg Oral Med Oral Pathol Oral Radiol Endod* 97, **2004**; pp. 398–403.

[9] SJ Shim, JI Lee, SH Baek and SS Lim, Tissue levels of matrix metalloproteinases in pulps and periopical lesons, *J Endod* 28, **2002**; pp. 313–315.

[10] H Gusman, RB Santana and M Zehnder, Matrix metalloproteinases levels and gelatinolytic activity in clinically health and inflamed human dental pulps, *Eur J Oral Sci* 110, **2002**; pp. 353–357.

[11] J.M. Delaisse, M.T. Engsig, V. Everts, M. del Carmen Ovejero, M. Ferreras, L. Lund, T.H. Vu, Z. Werb, B. Winding, A. Lochter, M.A. Karsdal, T. Troen, T. Kirkegaard, T. Lenhard, A.M. Heegaard, L. Neff, R. Baron and N.T. Foged , Proteinases in bone resorption: Obvious and less obvious roles. *Clin Chim Acta* 291, **2000**; pp. 223–234.

[12] V. Everts, J.M. Delaisse, W. Korper and W. Beertsen , Cysteine proteinases and matrix metalloproteinases play distinct roles, in the subosteoclastic resorption zone. *J Bone Miner Res* 13 , **1998**; pp. 1420–1430.

[13] V. Everts, J.M. Delaisse, W. Korper, A. Niehof, G. Vaes and W. Beertsen , Degradation of collagen in the bone-resorbing compartment underlying the osteoclast involves both cysteine-proteinases and matrix metalloproteinases. *J Cell Physiol* 150, **1992**; pp. 221–231.

[14] V. Everts, W. Korper, D.C. Jansen, J. Steinfort, I. Lammerse, S. Heera, A.J. Docherty and W. Beertsen , Functional heterogeneity of osteoclasts: Matrix metalloproteinases participate in osteoclastic resorption of calvarial bone but not in resorption of long bone. *FASEB J* 13, **1999**; pp. 1219–1230.

[15] P.A. Hill, A.J. Docherty, K.M. Bottomley, J.P. O'Connell, J.R. Morphy, J.J. Reynolds and M.C. Meikle , Inhibition of bone resorption in vitro by selective inhibitors of gelatinase and collagenase. *Biochem J* 308, **1995**; pp. 167–175.

[16] P.A. Hill, G. Murphy, A.J. Docherty, R.M. Hembry, T.A. Millican, J.J. Reynolds and M.C. Meikle , The effects of selective inhibitors of matrix metalloproteinases (MMPs) on bone resorption and the identification of MMPs and TIMP-1 in isolated osteoclasts. *J Cell Sci* 107, **1994**; pp. 3055–3064.

[17] K. Kusano, C. Miyaura, M. Inada, T. Tamura, A. Ito, H. Nagase, K. Kamoi and T. Suda , Regulation of matrix metalloproteinases (MMP-2, -3, -9, and -13) by interleukin-1 and interleukin-6

in mouse calvaria: Association of MMP induction with bone resorption. *Endocrinology* 139, **1998**; pp. 1338–1345.

[18] K. Tezuka, K. Nemoto, Y. Tezuka, T. Sato, Y. Ikeda, M. Kobori, H. Kawashima, H. Eguchi, Y. Hakeda and M. Kumegawa , Identification of matrix metalloproteinase 9 in rabbit osteoclasts. *J Biol Chem* 269, **1994**; pp. 15006–15009.

[19] K. Tezuka, Y. Tezuka, A. Maejima, T. Sato, K. Nemoto, H. Kamioka, Y. Hakeda and M. Kumegawa , Molecular cloning of a possible cysteine proteinase predominantly expressed in osteoclasts. *J Biol Chem* 269, **1994**; pp. 1106–1109.

[20] S. Bord, A. Horner, R.M. Hembry, J.J. Reynolds and J.E. Compston , Distribution of matrix metalloproteinases and their inhibitor, TIMP-1, in developing human osteophytic bone. *J Anat* 191**, 1997**; pp. 39–48.

[21] Y. Okada, K. Naka, K. Kawamura, T. Matsumoto, I. Nakanishi, N. Fujimoto, H. Sato and M. Seiki , Localization of matrix metalloproteinase 9 (92-kilodalton gelatinase/type IV COLLAGENASE = gelatinase B) in osteoclasts: Implications for bone resorption. *Lab Invest* 72, **1995**; pp. 311–322.

[22] P. Reponen, C. Sahlberg, C. Munaut, I. Thesleff and K. Tryggvason , High expression of 92-kD type IV collagenase (gelatinase B) in the osteoclast lineage during mouse development. *J Cell Biol* 124, **1994**; pp. 1091–1102.

[23] D.P. Rice, H.J. Kim and I. Thesleff , Detection of gelatinase B expression reveals osteoclasticbone resorption as a feature of early calvarial bone development. *Bone* 21, **1997**; pp. 479–486.

[24] L. Blavier and J.M. Delaisse , Matrix metalloproteinases are obligatory for the migration of preosteoclasts to the developing marrow cavity of primitive long bones. *J Cell Sci* 108, **1995**; pp. 3649–3659.

[25] P. Saftig, E. Hunziker, O. Wehmeyer, S. Jones, A. Boyde, W. Rommerskirch, J.D. Moritz, P. Schu and K. von Figura , Impaired osteoclastic bone resorption leads to osteopetrosis in cathepsin-K-deficient mice. *Proc Natl Acad Sci USA* 95, 1998; pp. 13453–13458.

[26] M.T. Engsig, Q.J. Chen, T.H. Vu, A.C. Pedersen, B. Therkidsen, L.R. Lund, K. Henriksen, T. Lenhard, N.T. Foged, Z. Werb and J.M. Delaisse , Matrix metalloproteinase 9 and vascular endothelial growth factor are essential for osteoclast recruitment into developing long bones. *J Cell Biol* 151, **2000**; pp. 879–890.

[27] Wang, X. and Ni, Q. Determination of Cortical Bone Porosity and Pore size Distribution Using a Field NMR Approach, *J. Orthop. Res*. **2003**;21(2): 312-319.

[28] Ni, Q., King, J.D. and Wang, X. Characterization of Human Bone StructureChanges By Low Field NMR, Measurement Science and Technology, **2004**;15:58 – 66.

[29] Brownstein, K. R., and Tarr, C. E. **1979** Importance of Classical Diffusion in NMR Studies of Water in Biological Cells, *Phys. Rev. A*. 19 2446.

[30] Ni, Q. and Nicolella, D.P. The Characterization of Human Cortical Bone Microdamage by Nuclear Magnetic Resonance. *Measurement Science and Technology*, **2005**;16: 659-668.

[31] Ni, Q., Nyman, J.S., Wang, X., De Los Santos, A., and Nicolella, D.P., Assessment of Water Distribution Changes in Human Cortical Bones by Nuclear Magnetic Resonance. *Measurement*

Science and Technology (Institute of Physics(IOP)), **2007**;18: 715-723.

[32] Carr, H.Y., and Purcell, E. M., Effects of Diffusion on Free Precession in Nuclear Magnetic Resonance Experiments. *Phys. Rev*. **1954**;904**(3):** 630.

[33] Meiboom, S., and Gill, D., Modified Spin-Echo Method for Measuring Nuclear Relaxation Times. *Rev. Sci. Inst*. 29**,** 688, **1958**.

[34] Ni, Q and Chen, S. "Assessment of Structural Changes of Human Teeth by Low-field Nuclear magnetic Resonance (NMR)" IOP (Institute of Physics) Electronic Journal *Measurement Science and Technology*, December 2009. (Print publication: Issue 1 Jan. **2010**).

[35] Vu T, Shipley J, Bergers G, Berger J, Helms J, Hanahan D, Shapiro S, Senior R, Werb Z MMP-9/gelatinase B is a key regulator of growth plate angiogenesis and apoptosis of hypertrophic chondrocytes. Cell, **1998**;93:411–422.